Mathematics in Applied Sciences and Engineering
Volume **4**, Number **4**, December **2023**, pp.**285-306**
https://ojs.lib.uwo.ca/mase
https://doi.org/10.5206/mase/16743

ASSESSING THE IMPACT OF HOST PREDATION WITH HOLLING II RESPONSE ON THE TRANSMISSION OF CHAGAS DISEASE

JIAHAO JIANG, DAOZHOU GAO, JIAO JIANG, AND XIAOTIAN WU

Abstract. Chagas disease is a zoonosis caused by the protozoan parasite *Trypanosoma cruzi* and transmitted by a broad range of blood-sucking triatomine species. Recently, it is recognized that the parasite can also be transmitted by host ingestion. In this paper, we propose a Chagas disease model incorporating two transmission routes of biting-defecation and host predation between vectors and hosts with Holling II functional response. The basic reproduction number $\mathcal{R}_v$ of triatomine population and basic reproduction numbers $\mathcal{R}_0$ of disease population are derived analytically, and it is shown that they are insufficient to serve as threshold quantities to determine dynamics of the model. Our results have revealed the phenomenon of bistability, with backward and forward bifurcations. Specifically, if $\mathcal{R}_v > 1$, the dynamic is rather simple, namely, the disease-free equilibrium is globally asymptotically stable as $\mathcal{R}_0 < 1$ and a unique endemic equilibrium is globally asymptotically stable as $\mathcal{R}_0 > 1$. However, if $\mathcal{R}_v < 1$, there exists a backward bifurcation with one unstable and one stable positive vector equilibria, and bistability phenomenon occurs, revealing that different initial conditions may lead to disease extinction or persistence even if the corresponding $\mathcal{R}_0 > 1$. In conclusion, predation transmission in general reduces the risk of Chagas disease, whilst it makes the complexity of Chagas disease transmission, requiring an integrated strategy for the prevention and control of Chagas disease.

1. Introduction

Chagas disease is a vector-borne disease caused by the protozoan parasite *Trypanosoma cruzi (T. cruzi)*, transmitted by a broad range of blood-sucking triatomine species with approximately 140 species in the world [13]. Humans infected with *T. cruzi* can cause severe life-threatening cardiac and gastrointestinal illness and currently no vaccine is available. It is reported that 21 countries across Latin America are endemic, around 6-7 million people in the world are infected with *T. cruzi* and around 75 million people are at risk of infection [19]. Moreover, around 30,000 new cases and approximately 12,000 deaths are present per year [19]. Accordingly, the prevention and control of Chagas disease remains a great challenge.

The transmission of the *T. cruzi* parasites is mainly attributed to the contact between triatomine vectors and their reservoir hosts. Generally, *T. cruzi*-infected triatomine bugs feed on reservoir hosts' blood, deposit their feces with *T. cruzi* parasites on the skin of hosts, then these parasites penetrate the hosts' body bloodstream through the bite wound sites due to hosts' scratching or rubbing or other means [13]. Due to the zoonotic nature and a wide geographical range of living settings, a number of human and non-human primates host species can serve as nutritional resources for triatomine bugs, such as rodents, marsupials, dogs, cats and so on [6, 8, 10]. This contact can render animal population or triatomine bugs infectious when susceptible hosts are fed by *T. cruzi*-infected triatomine bugs,

Received by the editors 20 August 2023; accepted 3 November 2023; published online 8 November 2023.
2020 *Mathematics Subject Classification.* Primary 34A34, 34D20; Secondary 92C60, 92D30.
Key words and phrases. Chagas disease, *Trypanosoma cruzi*, predation transmission, bistability, backward bifurcation.

or susceptible triatomines feed on infected hosts. The interplay between animals and vectors can potentially impact the prevalence of Chagas-positive human population.

It is definitive that a broad diversity of host species is one of the most important factors for the complexity of Chagas disease's control and prevention. Nevertheless, it is worth to point out that many of them like raccoons and opossums are omnivorous with their diets including plants, small animals, insects and armadillos and so on [6, 8]. Particularly, dogs can consume triatomine bugs and are able to maintain the *T. cruzi* transmission in the absence of other hosts [8]; monkey can become infected when they have eaten *T. cruzi* infected triatomine bugs [11]. These evidences indicate that there is an additional transmission route of Chagas disease, called predation transmission. Studies [6, 11] also suggest that parasite transmission through host predation may be an effective pathway for the Chagas-parasite persistence, and may even more efficient than the traditional biting-defecation transmission mechanism. However, to the best of our knowledge, how host predation and its infection impact on the *T. cruzi* transmission has not been fully understood. This allows us to explore the potential influence of predator-prey mechanism on the persistence of Chagas disease, which is crucial for the control and prevention of Chagas disease.

Predation transmission of Chagas disease is not rare in the literature. Some experimental works have manifested that carnivores such as raccoons and opossums can become infected when they ingest infected triatomines [10, 16, 22]. Some investigators have used different Holling-type functional responses to mimic the host predation and infection process [5, 6, 11]. These pieces of evidences have been unraveled the potential significance of predation behavior on the transmission of Chagas disease.

Significant progress has been made on the dynamics and risk assessment of Chagas disease. Early studies have been focused on the vector-host interaction considering simple vectors' biting and defecation transmission while having distinct clinical symptoms of humans as acute and chronic phases [7, 30]. In subsequent studies, additional different transmission routes such as blood transfusion [31], oral or congenital transmission [5, 3], and different Chagas-related parasites like *T. cruzi* and *T. rangeli* [4, 32, 33] were integrated into models to examine these factors on the transmission of Chagas disease. The delay effect of gestation or growth of triatomine bugs on the transmission of Chagas disease have been also studied [5, 25]. Many researchers have concentrated on control strategies, like periodic/non-periodic insecticide spraying, to evaluate their effectiveness in combating Chagas disease [24, 25]. However, the impact of animal hosts' predation of triatomine vectors on the transmission of Chagas-parasite has not been fully understood so far, which draws our attention in this study.

The paper is organized as follows. In section 2, we formulate a mathematical model of Chagas disease with an emphasis on vector's predation by animal hosts. In section 3, we establish the threshold dynamics in terms of basic reproduction number of vector population and basic reproduction numbers of disease population. In section 4, numerical simulations are performed to reveal the effect of predation on the transmission and control of Chagas disease. The paper ends with a brief conclusion and discussion.

2. **The Model**

Since both triatomine bugs and hosts (animals) infected with *T. cruzi* generally lead to life-long carriers, both vector and host populations are divided into susceptible ($S_j(t)$) and infected ($I_j(t)$) classes, where $j = v, h$. Moreover, mortality of animals infected with *T. cruzi* is limited, thus no disease-induced death is assumed for host population. For simplicity, we further assume hosts grow and die at the same rate μ_h, with an aim to maintain the total number of host population as a constant, denoted by N_h.

Generally, the reproduction of insects is influenced by ecological environmental source, namely, increases linearly at small densities, decreases due to intraspecific competition, and then drops significantly

at very large densities as a consequence of the available environmental resources [21]. Following [32, 33], the new susceptible triatomine population at time t grows at a Ricker-type function

$$b(N_v(t)) = r_v N_v(t) e^{-\sigma N_v(t)},$$

where $N_v(t) = S_v(t) + I_v(t)$ is the total number of vectors at time t, r_v is the maximal number of offspring produced by per adult triatomine and σ measures the density-dependent strength.

Denote by a the number of bites per bug per unit time, then susceptible triatomines become infected through the bites on the infected hosts at a rate $ba\frac{I_h(t)}{N_h}S_v(t)$, where b is the transmission probability from infected hosts to susceptible triatomines per bite. As we mentioned in introduction, animal hosts can ingest on triatomine insects, hence both susceptible and infected triatomines can decay at rates

$$\frac{mN_v(t)}{n+N_v(t)}\frac{S_v(t)}{N_v(t)}N_h \text{ and } \quad \frac{mN_v(t)}{n+N_v(t)}\frac{I_v(t)}{N_v(t)}N_h,$$

respectively, where Holling-II functional response mimics the predator-prey mechanism, m is the maximum predation rate per host, and n is the half-saturation constant. Thus, dynamic of triatomine population is governed by

$$\begin{cases} S_v'(t) = r_v N_v(t) e^{-\sigma N_v(t)} - ba\dfrac{I_h(t)}{N_h}S_v(t) - \dfrac{mS_v(t)}{n+N_v(t)}N_h - \mu_v S_v(t), \\ I_v'(t) = ba\dfrac{I_h(t)}{N_h}S_v(t) - \dfrac{mI_v(t)}{n+N_v(t)}N_h - \mu_v I_v(t), \end{cases}$$

where μ_v is the natural death rate of triatomines.

For the host population, there are two routes that susceptible hosts ($S_h(t)$) can become infected. On the one hand, susceptible hosts become infected at a rate $caI_v(t)\frac{S_h(t)}{N_h}$, when they are bitten by those infected triatomine bugs, where c is the transmission probability from infected vectors to susceptible hosts per bite. On the other hand, the susceptible hosts become infected when they catch and consume infected insects at a rate

$$p\frac{mN_v(t)}{n+N_v(t)}\frac{I_v(t)}{N_v(t)}S_h(t),$$

where p is the transmission probability per predation. Hence, dynamics of host population are governed by

$$\begin{cases} S_h'(t) = \mu_h\big(S_h(t)+I_h(t)\big) - ca\dfrac{I_v(t)}{N_h}S_h(t) - p\dfrac{mI_v(t)}{n+N_v(t)}S_h(t) - \mu_h S_h(t), \\ I_h'(t) = ca\dfrac{I_v(t)}{N_h}S_h(t) + p\dfrac{mI_v(t)}{n+N_v(t)}S_h(t) - \mu_h I_h(t). \end{cases}$$

Since the total number of hosts is constant, then the final closed system describing the interaction between triatomine bugs and animal hosts is governed by

$$\begin{cases} S_v'(t) = r_v N_v(t) e^{-\sigma N_v(t)} - ba\dfrac{I_h(t)}{N_h}S_v(t) - \dfrac{mS_v(t)}{n+N_v(t)}N_h - \mu_v S_v(t), \\ I_v'(t) = ba\dfrac{I_h(t)}{N_h}S_v(t) - \dfrac{mI_v(t)}{n+N_v(t)}N_h - \mu_v I_v(t), \\ I_h'(t) = ca\dfrac{I_v(t)}{N_h}\big(N_h - I_h(t)\big) + p\dfrac{mI_v(t)}{n+N_v(t)}\big(N_h - I_h(t)\big) - \mu_h I_h(t), \end{cases} \tag{2.1}$$

with the initial condition

$$S_v(0) \geq 0, \quad I_v(0) \geq 0, \quad I_h(0) \geq 0. \tag{2.2}$$

Note that all model parameters are nonnegative in terms of biological meanings, and their ranges are given in Table 1. The flowchart of the model (2.1-2.2) is presented in Figure 1.

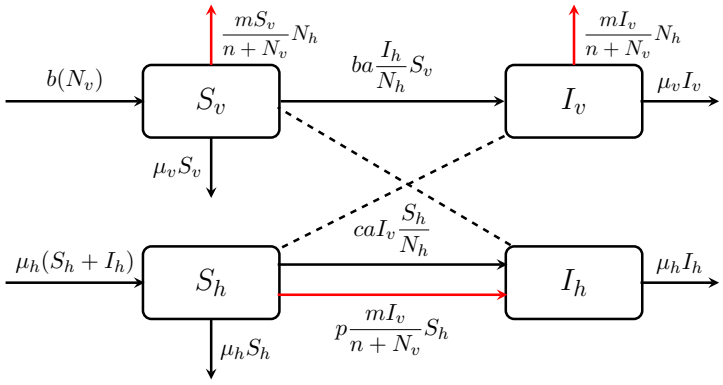

FIGURE 1. Flowchart of model (2.1) with both biting-defecation and predation transmission routes

TABLE 1. Parameter description and reference

Parameter	Description	Range/Value	Reference
r_v	the maximal number of offspring that a triatomine bug can produce per unit time	$[0.0274, 0.7714]$/day	[1, 12, 14]
a	number of bites per bug per unit time	$[0.2, 33]$/day	[12, 14, 32]
b	transmission probability from infected hosts to susceptible bugs per bite	$[0.00271, 0.06]$	[12, 14, 28, 32]
c	transmission probability from infected bugs to susceptible hosts per bite	$[0.00026, 0.49]$	[1, 12, 28]
σ	density-dependency strength measuring the bugs reproduction	$(0, 0.1)$	[32]
p	transmission probability per predation from infected vectors to susceptible hosts	$(0, 1)$	in this study
μ_v	natural death rate per vector	$[0.0045, 0.0083]$/day	[1, 12, 28]
μ_h	natural death rate per host	$[0.00014, 0.0025]$/day	[1, 12, 18]
N_h	total number of hosts	[100,700]	Assumed
n	half-saturation constant for predation	varied	[5]
m	maximum predation rate	varied	[5]

Proposition 2.1. *System (2.1) has a unique, nonnegative and bounded solution for all $t \geq 0$, with initial value lying in*

$$\mathcal{D} = \left\{ (S_v, I_v, I_h) \in \mathbb{R}^3_+ \middle| S_v + I_v \leq \frac{r_v}{\mu_v \sigma e}, I_h \leq N_h \right\}.$$

Proof. Summing up the first and second equations in system (2.1) yields

$$N_v'(t) \leq r_v N_v(t) e^{-\sigma N_v(t)} - \mu_v N_v(t) \leq \frac{r_v}{\sigma e} - \mu_v N_v(t), \tag{2.3}$$

where the fact of $xe^{-\sigma x} \leq \frac{1}{\sigma e}$ for $x \geq 0$ is used for the inequality. Thus, $\mathcal{D}$ is a positive invariant set of model (2.1).

Since the vector field generated by the right side of (2.1) is continuously differentiable in $\mathcal{D}$, there exists a unique solution for all time $t \geq 0$. The nonnegativity of (2.1) with the initial value in $\mathcal{D}$ directly follows from Theorem 5.2.1 in [23]. The boundedness of S_v and I_v directly follows from Eq. (2.3). □

3. Mathematical Analysis

In order to investigate the disease dynamics of model (2.1), we first consider the dynamics of triatomine population.

3.1. Vector Population Dynamics.

Adding the first and second equations in (2.1) leads to

$$\begin{aligned} N_v'(t) &= r_v N_v(t) e^{-\sigma N_v(t)} - \frac{m N_v(t)}{n + N_v(t)} N_h - \mu_v N_v(t) \\ &\triangleq f(N_v(t)) = N_v(t) f_1(N_v(t)), \end{aligned} \tag{3.1}$$

where

$$f_1(N_v) = r_v e^{-\sigma N_v} - \frac{m N_h}{n + N_v} - \mu_v, \tag{3.2}$$

with the positive invariant set of (3.1) as $\mathcal{D}_v = \{N_v \in \mathbb{R}_+ | \, 0 \le N_v \le \frac{r_v}{\sigma \mu_v e}\}$.

Applying the next-generation matrix method [29] at triatomine-free equilibrium $N_{v0}^* = 0$, the basic reproduction number of triatomine population is

$$\mathcal{R}_v = \frac{r_v}{\frac{m N_h}{n} + \mu_v} < \frac{r_v}{\mu_v}. \tag{3.3}$$

indicating host predation reduces the vector reproduction number $\mathcal{R}_v$.

3.1.1. *Equilibrium Analysis.*

The positive equilibrium of system (3.1) is equivalent to seek for the positive roots of $f_1(N_v) = 0$. The derivative of f_1 *w.r.t.* N_v is

$$f_1'(N_v) = \frac{m N_h}{(n + N_v)^2} \Big(1 - g(N_v)\Big), \tag{3.4}$$

where

$$g(N_v) = \frac{\sigma r_v}{m N_h} (n + N_v)^2 e^{-\sigma N_v}. \tag{3.5}$$

The mathematical properties of f_1 and g play a crucial role in determining the existence and number of positive equilibria of system (3.1).

Lemma 3.1. *The function g defined in Eq. (3.5) has the following properties:*

(i) *if $\sigma n \ge 2$, then $g(N_v)$ is strictly decreasing from $g(0) > 0$ to zero.*

(ii) *if $0 < \sigma n < 2$, then there is a unique stationary point $\widetilde{N}_v = \frac{2 - \sigma n}{\sigma} > 0$ such that $g(N_v)$ increases first at $[0, \widetilde{N}_v)$, reaches a maximum value $g_{max} \triangleq g(\widetilde{N}_v)$, and then decreases to zero at $(\widetilde{N}_v, +\infty)$.*

Proof. Clearly, $g(0) = \sigma n \frac{r_v}{m N_h / n} > 0$, and

$$g'(N_v) = -\frac{\sigma^2 r_v}{m N_h} (n + N_v) e^{-\sigma N_v} \left(N_v - \frac{2 - \sigma n}{\sigma}\right). \tag{3.6}$$

It is obvious that: *(i)* if $\sigma n \ge 2$, $g'(N_v) < 0$ for $N_v \ge 0$; *(ii)* if $0 < \sigma n < 2$, there admits $\widetilde{N}_v = \frac{2 - \sigma n}{\sigma} > 0$ such that $g'(\widetilde{N}_v) = 0$, $g'(N_v) > 0$ for $N_v \in [0, \widetilde{N}_v)$ and $g'(N_v) < 0$ for $N_v \in (\widetilde{N}_v, +\infty)$, and $g_{max} \triangleq \max_{N_v \in [0, \infty)} g(N_v) = g(\widetilde{N}_v) > g(0)$. □

Based on Eqs. (3.2)-(3.5) and Lemma 3.1, we have the following result on the equilibrium of system (3.1).

Theorem 3.2. *For system (3.1), we have*

(i) *If $\mathcal{R}_v > 1$, there admits a unique positive equilibrium N_v^*.*

(ii) *If $\mathcal{R}_v < 1$, there are up to two positive equilibria. Specifically,*

(a) *if* $0 < \sigma n < 1 - \frac{\mu_v}{r_v}$ *and* $m_l < m < m_u$, *where*

$$m_l = \frac{n(r_v - \mu_v)}{N_h} \quad \text{and} \quad m_u = \frac{\mu_v}{\sigma N_h} \frac{\left(1 - W_0(\frac{\mu_v}{r_v} e^{1-\sigma n})\right)^2}{W_0(\frac{\mu_v}{r_v} e^{1-\sigma n})},$$

there are two positive equilibria $N^*_{v\pm}$ *satisfying*

$$N^*_{v^-} < \frac{2 - \sigma n}{\sigma} < N^*_{v^+}.$$

(b) *if* $0 < \sigma n < 1 - \frac{\mu_v}{r_v}$ *and* $m = m_u$, *there is one unique positive equilibrium*

$$N^*_{v\pm} \triangleq \bar{N}^*_v = \sqrt{\left(\frac{mN_h}{2\mu_v}\right)^2 + \frac{mN_h}{\sigma\mu_v}} - \left(\frac{mN_h}{2\mu_v} + n\right).$$

(c) *if otherwise, there is no positive equilibrium.*

Remark 3.1. The condition for the two equilibria if $\mathcal{R}_v < 1$ is equivalent to

$$0 < \sigma n < 2, \ g(0) \le 1 < g_{max},$$

and there is a $\widetilde{N}_{v1} < (2 - \sigma n)/\sigma$ such that

$$f_1(\widetilde{N}_{v1}) > 0, \ f_1'(\widetilde{N}_{v1}) = 0.$$

The proofs of Theorem 3.2 and Remark 3.1 are provided in Appendix A. Figures 2-3 present an intuitive observation of the existence and number of positive equilibria of system (3.1) in case of $\mathcal{R}_v > 1$ and $\mathcal{R}_v < 1$, respectively.

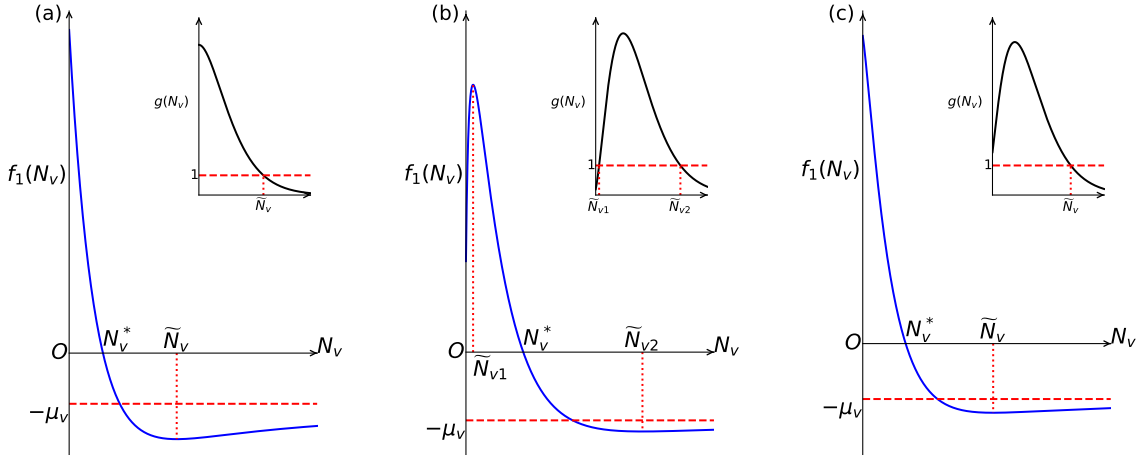

FIGURE 2. The unique positive equilibrium of system (3.1) if $\mathcal{R}_v > 1$. (a) $\sigma n \ge 2$; (b) $0 < \sigma n < 2$ and $g(0) < 1$; (c) $0 < \sigma n < 2$ and $g(0) \ge 1$.

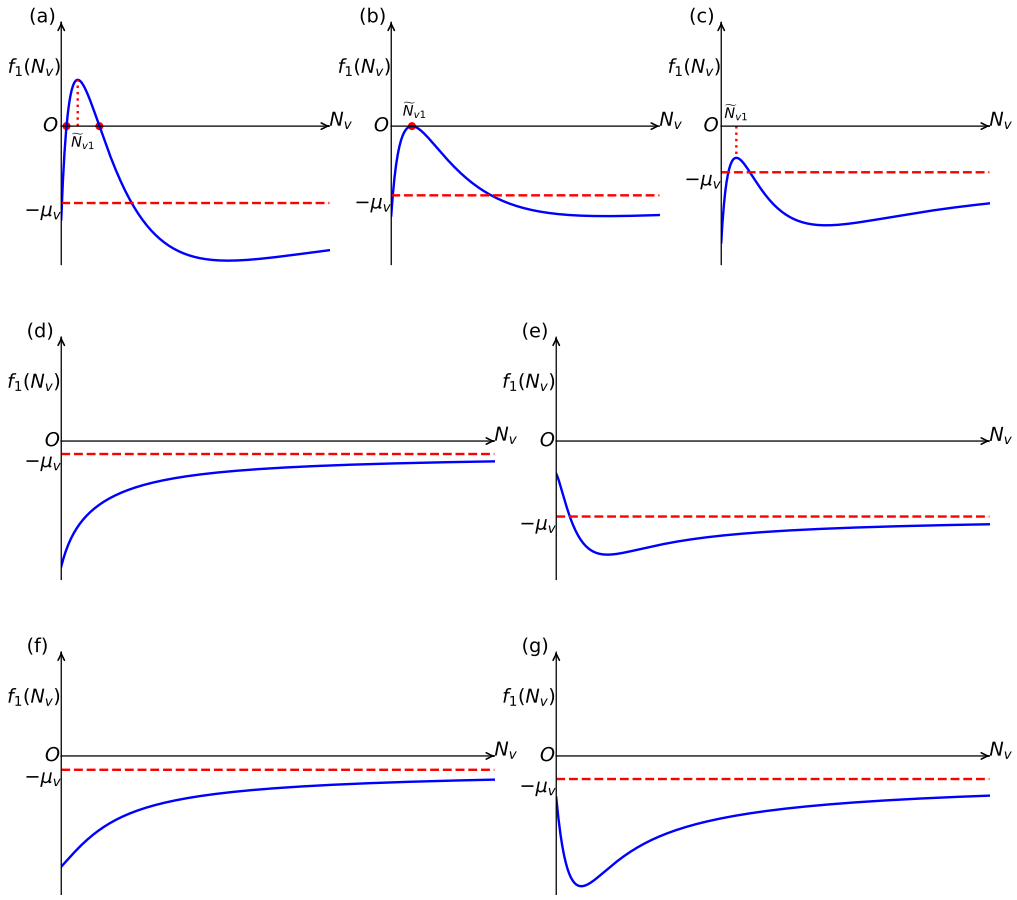

FIGURE 3. The number of positive roots for $f_1(N_v) = 0$ when $\mathcal{R}_v < 1$. (a) $0 < \sigma n < 2$, $g(0) \leq 1 < g_{max}$ and $f_1(\widetilde{N}_{v1}) > 0$; (b) $0 < \sigma n < 2$, $g(0) \leq 1 < g_{max}$ and $f_1(\widetilde{N}_{v1}) = 0$; (c) $0 < \sigma n < 2$, $g(0) \leq 1 < g_{max}$ and $f_1(\widetilde{N}_{v1}) < 0$; (d) $0 < \sigma n < 2$ and $g_{max} \leq 1$; (e) $0 < \sigma n < 2$ and $g(0) > 1$; (f) $\sigma n \geq 2$ and $g(0) \leq 1$; (g) $\sigma n \geq 2$ and $g(0) > 1$.

3.1.2. *Stability and Bifurcation Analysis.*

Theorem 3.3. *For system (3.1), we have*

(i) *If $\mathcal{R}_v > 1$, then N_v^* is globally asymptotically stable (GAS) and N_{v0}^* is unstable in $\mathcal{D}_v$.*
(ii) *If $\mathcal{R}_v < 1$, then N_{v0}^* and N_{v+}^* is locally asymptotically stable (LAS) and N_{v-}^* is unstable in $\mathcal{D}_v$.*

Proof. The stability can be obtained by Proposition 3.5.1 [15] since

$$N_v''(t) = f'(N_v) = f_1(N_v) + N_v f_1'(N_v).$$

(i) If $\mathcal{R}_v > 1$,

$$f'(N_v^*) = N_v^* f_1'(N_v^*) < 0,\ f'(N_{v0}^*) = f_1(0) > 0,$$

indicating N_v^* is GAS and N_{v0}^* is unstable in $\mathcal{D}_v$.

(ii) If $\mathcal{R}_v < 1$,

$$f'(N_{v-}^*) = N_{v-}^* f_1'(N_{v-}^*) > 0,\ f'(N_{v+}^*) = N_{v+}^* f_1'(N_{v+}^*) < 0,\ f'(N_{v0}^*) = f_1(0) < 0,$$

indicating that $N^*_{v^-}$ is unstable, and both N^*_{v0} and $N^*_{v^+}$ is LAS in $\mathcal{D}_v$. □

Theorem 3.4. *System (3.1) experiences a backward bifurcation when $\mathcal{R}_v < 1$, and undergoes a saddle-node bifurcation at the positive equilibrium $\bar{N}^*_v$ as the parameter m passes through $m = m_u$.*

Proof. We consider the parameter m as a bifurcation parameter. It follows from Theorem 3.2 that there is a bifurcation occurring at the unique positive equilibrium $\bar{N}^*_v$ when $\mathcal{R}_v < 1$, $0 < \sigma n < 1 - \frac{\mu_v}{r_v}$ and $m = m_u$.

Denote by ω_1 and ω_2 the right and left eigenvectors corresponding to the zero eigenvalue at $\bar{N}^*_v$, respectively, and we can readily obtain $\omega_1 = \omega_2 = 1$, and then transversality conditions at $\bar{N}^*_v$ and m_u are

$$\omega_2^T f_m(\bar{N}^*_v, m_u) = -\frac{N_h \bar{N}^*_v}{n + \bar{N}^*_v} \neq 0,$$
$$\omega_2^T \left[D^2 f(\bar{N}^*_v, m_u)(\omega_1, \omega_1) \right] = -\frac{m_u N_h \bar{N}^*_v}{(n + \bar{N}^*_v)^3} \left(1 + \frac{\mu_v}{r_v e^{-\sigma \bar{N}^*_v}} \right) \neq 0.$$

It follows from Sotomayor's theorem [20] that system (3.1) experiences a saddle-node bifurcation at $\bar{N}^*_v$ as m passes through m_u. □

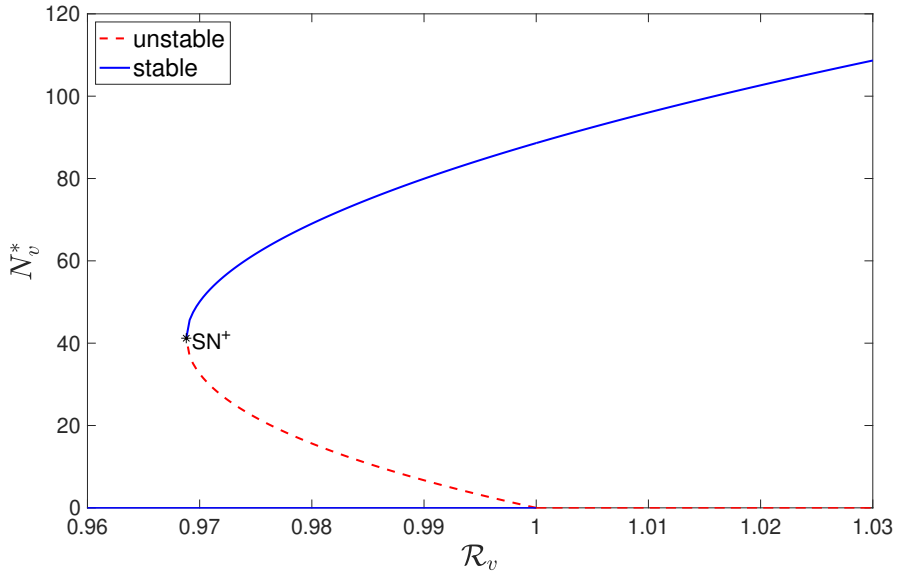

FIGURE 4. Backward bifurcation of model (3.1) in terms of $\mathcal{R}_v$, where $N_h = 200, \sigma = 0.0001, r_v = 0.0274, \mu_v = 0.0083$ and $n = 5228$. Blue solid lines indicate stable equilibrium, red dashed lines indicate unstable equilibrium. Notation 'SN^+' represents the saddle-node bifurcation.

Figure 4 shows the backward bifurcation of system (3.1) in terms of $\mathcal{R}_v$. It is noticed that, as $\mathcal{R}_v < 1$, there exists one stable ($N^*_{v^+}$) and one unstable ($N^*_{v^-}$) vector equilibria. Biologically, this implies that a small perturbation in model parameters or initial conditions may result in a significant deviation in the vector's dynamics.

Remark 3.2. In fact, without the host predation on insects, the dynamics of vector population are rather simple. Namely, there is a unique vector-free equilibrium if $\mathcal{R}_v < 1$ and a unique positive vector equilibrium which is globally asymptotically stable if $\mathcal{R}_v > 1$. However, with the presence of host predation, the backward bifurcation occurs as shown in Fig. 4, implying the host predation on insects makes the complexity of the dynamics of vector population, hence the complexity of proposed Chagas disease model (2.1).

3.2. **Threshold Dynamics of System (2.1).**

3.2.1. *Basic Reproduction Numbers.* It follows from Theorem 3.2 that system (2.1) have the disease-free equilibria (DFE):

$$E_{b^\pm} = (N^*_{v^\pm}, 0, 0) \text{ if } \mathcal{R}_v < 1$$

and

$$E_b = (N^*_v, 0, 0) \text{ if } \mathcal{R}_v > 1.$$

Using the next-generation matrix method [29], the rates of appearance of new infections and transition of individuals are

$$\mathscr{F} = \begin{pmatrix} ba\frac{I_h(t)}{N_h}S_v(t) \\ caI_v(t)\frac{N_h - I_h(t)}{N_h} + p\frac{mI_v(t)}{n+N_v(t)}\big(N_h - I_h(t)\big) \end{pmatrix}$$

and

$$\mathscr{V} = \begin{pmatrix} \frac{mI_v(t)}{n+N_v(t)}N_h + \mu_v I_v(t) \\ \mu_h I_h(t) \end{pmatrix},$$

respectively. So, the new incidence and transition matrices at $(\widetilde{S}_v, 0, 0)$ are

$$F = \begin{pmatrix} 0 & ba\frac{\widetilde{S}_v}{N_h} \\ ca + p\frac{mN_h}{n+\widetilde{S}_v} & 0 \end{pmatrix}, \quad \text{and} \quad V = \begin{pmatrix} \frac{mN_h}{n+\widetilde{S}_v} + \mu_v & 0 \\ 0 & \mu_h \end{pmatrix},$$

respectively, and $\widetilde{S}_v$ could be $N^*_{v^\pm}$ or N^*_v. Hence, the basic reproduction number of model (2.1) is

$$\begin{aligned} \mathcal{R}_0(\widetilde{S}_v) &= \rho(FV^{-1}) = \sqrt{\frac{ca}{\mu_h}\frac{ba\widetilde{S}_v}{(\frac{mN_h}{n+\widetilde{S}_v} + \mu_v)N_h} + \frac{p\frac{mN_h}{n+\widetilde{S}_v}}{\mu_h}\frac{ba\widetilde{S}_v}{(\frac{mN_h}{n+\widetilde{S}_v} + \mu_v)N_h}}, \\ &\equiv \sqrt{\mathcal{R}_b + \mathcal{R}_p}, \end{aligned} \tag{3.7}$$

where $\mathcal{R}_b$ and $\mathcal{R}_p$ are the reproduction numbers caused by vector's biting-defecation and host's predation transmission routes, respectively.

Following Eq. (3.7), we have

$$\mathcal{R}_0(N^*_{v^-}) < \mathcal{R}_0(N^*_{v^+}) < \mathcal{R}_0(N^*_v).$$

These formulas and relationship provide the threshold conditions for the endemicity of Chagas epidemic in population where the model (2.1) is at DFE.

3.2.2. *Existence and Stability of Endemic Equilibria.* We will explore the threshold dynamics of system (2.1) in terms of $\mathcal{R}_v$ and $\mathcal{R}_0$.

Theorem 3.5. *If $\mathcal{R}_v > 1$, system (2.1) has up to three equilibria:*

$$E_0 = (0, 0, 0),\ E_b = (N^*_v, 0, 0),\ E_e = (S^*_v, I^*_v, I^*_h).$$

Moreover, we have

(i) *If $\mathcal{R}_0(N^*_v) < 1$, only E_0 and E_b exist. Moreover, E_0 is unstable and E_b is GAS in $\mathcal{D}$.*

(ii) *If $\mathcal{R}_0(N_v^*) > 1$, all E_0, E_b and E_e exist. Moreover, both E_0 and E_b are unstable and E_e is GAS in $\mathcal{D}$.*

Proof. In case of $\mathcal{R}_v > 1$, it follows from Theorem 3.2 that N_v^* is GAS in $\mathcal{D}_v$. Results in [26, 27] indicate that the long-term dynamics of system (2.1) are equivalent to the following limiting system:

$$\begin{cases} I_v'(t) = ba\dfrac{I_h(t)}{N_h}\big(N_v^* - I_v(t)\big) - \dfrac{mI_v(t)}{n+N_v^*}N_h - \mu_v I_v(t), \\ I_h'(t) = caI_v(t)\dfrac{N_h - I_h(t)}{N_h} + p\dfrac{mI_v(t)}{n+N_v^*}\big(N_h - I_h(t)\big) - \mu_h I_h(t) \end{cases} \tag{3.8}$$

within a positive invariant set $\mathcal{D}_d = \{(I_v, I_h) \in \mathbb{R}_+^2 | \, 0 \le I_v \le N_v^*, \, 0 \le I_h \le N_h\}$. For simplicity, $\mathcal{R}_0$ is used in this portion instead of $\mathcal{R}_0(N_v^*)$.

(i) Suppose $\mathcal{R}_0 < 1$. It is clear that system (3.8) has a disease-free equilibrium $(0, 0)$. For its stability, let us construct a Lyapunov function:

$$V(I_v, I_h) = k_1 I_v + k_2 I_h,$$

where k_1 and k_2 are two positive constants to be determined later. Then, the total derivative of V along the solution of system (3.8) is

$$\begin{aligned} \frac{dV}{dt} &= k_1 I_v' + k_2 I_h' \\ &= k_1\left(ba\frac{I_h}{N_h}\Big(N_v^* - I_v\Big) - \frac{mI_v}{n+N_v^*}N_h - \mu_v I_v\right) \\ &\quad + k_2\left(caI_v\frac{N_h - I_h}{N_h} + p\frac{mI_v}{n+N_v^*}\Big(N_h - I_h\Big) - \mu_h I_h\right) \\ &= \Big(k_1\frac{ba}{N_h}N_v^* - k_2\mu_h\Big)I_h - \left[k_1\frac{ba}{N_h} + k_2\Big(\frac{ca}{N_h} + \frac{pm}{n+N_v^*}\Big)\right]I_v I_h \\ &\quad + \left[k_2\Big(ca + p\frac{mN_h}{n+N_v^*}\Big) - k_1\Big(\mu_v + \frac{mN_h}{n+N_v^*}\Big)\right]I_v. \end{aligned}$$

Choosing $k_1 = \mu_h$, $k_2 = \frac{ba}{N_h}N_v^*$, we obtain

$$\frac{dV}{dt} = \mu_h I_v\big(\mu_v + \frac{mN_h}{n+N_v^*}\big)\big(\mathcal{R}_0^2 - 1\big) - \frac{ba}{N_h}\left[\mu_h + \Big(\frac{ca}{N_h} + \frac{pm}{n+N_v^*}\Big)N_v^*\right]I_v I_h \le 0$$

due to $\mathcal{R}_0 < 1$. Moreover, we have $\frac{dV}{dt}(I_v, I_h) = 0$ if and only if $(I_v, I_h) = (0, 0)$. By LaSalle's invariance principle [2], $(0, 0)$ of system (3.8) is GAS in $\mathcal{D}_d$ if $\mathcal{R}_0 < 1$, indicating E_b of system (2.1) is GAS in $\mathcal{D}$ if $\mathcal{R}_0 < 1$ and $\mathcal{R}_v > 1$.

(ii) Suppose $\mathcal{R}_0 > 1$. Letting $I_v'(t) = 0$ and direct algebraic calculations lead to

$$0 < S_v^* = \frac{\alpha}{\alpha + I_h^*}N_v^* < N_v^*, \quad I_v^* = \frac{I_h^*}{N_h - I_h^*}\gamma > 0,$$

and

$$0 < I_h^* = \frac{\alpha\gamma}{N_v^* + \gamma}\big(\mathcal{R}_0^2 - 1\big) = N_h - \frac{(N_h + \alpha)\gamma}{N_v^* + \gamma} < N_h,$$

where

$$\alpha = \frac{\frac{mN_h}{n+N_v^*} + \mu_v}{ba/N_h}, \quad \gamma = \frac{\mu_h N_h}{ca + p\frac{mN_h}{n+N_v^*}} \quad \text{and} \quad S_v^* + I_v^* = N_v^*,$$

implying the existence of endemic equilibrium $E_e = (S_v^*, I_v^*, I_h^*)$.

We now examine the stability of (I_v^*, I_h^*) of model (3.8). The corresponding Jacobian matrix is

$$J\Big|_{(I_v^*,I_h^*)} = \begin{pmatrix} -\frac{ba}{N_h}I_h^* - \frac{mN_h}{n+N_v^*} - \mu_v & \frac{ba}{N_h}(N_v^* - I_v^*) \\ (\frac{ca}{N_h} + \frac{pm}{n+N_v^*})(N_h - I_h^*) & -\frac{ca}{N_h}I_h^* - \frac{pmI_v^*}{n+N_v^*} - \mu_h \end{pmatrix},$$

with

$$\text{tr } J\Big|_{(I_v^*,I_h^*)} = -\left(\frac{ba}{N_h}I_h^* + \frac{mN_h}{n+N_v^*} + \mu_v + \frac{ca}{N_h} + \frac{pmI_v^*}{n+N_v^*} + \mu_h\right) < 0,$$

and

$$\begin{aligned} \det J\Big|_{(I_v^*,I_h^*)} &= q\left(1 - \frac{(\frac{ca}{N_h} + \frac{pm}{n+N_v^*})(N_h - I_h^*)}{\frac{ca}{N_h}I_v^* + \frac{pmI_v^*}{n+N_v^*} + \mu_h} \frac{\frac{ba}{N_h}(N_v^* - I_v^*)}{\frac{ba}{N_h}I_h^* + \frac{mN_h}{n+N_v^*} + \mu_v}\right) \\ &\triangleq q\Big(1 - \frac{q_1}{q_2}\Big), \end{aligned}$$

where

$$q = \Big(\frac{ba}{N_h}I_h^* + \frac{mN_h}{n+N_v^*} + \mu_v\Big)\Big(\frac{ca}{N_h}I_v^* + \frac{pmI_v^*}{n+N_v^*} + \mu_h\Big) > 0.$$

Furthermore, we have

$$\begin{aligned} q_2 I_v^* I_h^* &= \left(\frac{ca}{N_h}I_v^* + \frac{pmI_v^*}{n+N_v^*} + \mu_h\right) I_h^* \left(\frac{ba}{N_h}I_h^* + \frac{mN_h}{n+N_v^*} + \mu_v\right) I_v^* \\ &= \left(\frac{ca}{N_h} + \frac{pm}{n+N_v^*}\right) N_h I_v^* \cdot \frac{ba}{N_h} N_v^* I_h^* \\ &> \left(\frac{ca}{N_h} + \frac{pm}{n+N_v^*}\right)(N_h - I_h^*) \cdot \frac{ba}{N_h}(N_v^* - I_v^*) \cdot I_v^* I_h^* \\ &= q_1 I_v^* I_h^*, \end{aligned}$$

where the equilibrium equation is used. Hence we obtain $q_2 > q_1$, implying

$$\det J\Big|_{(I_v^*,I_h^*)} > 0.$$

By Routh-Hurwitz criteria, both real parts of eigenvalues of $J\Big|_{(I_v^*,I_h^*)}$ are negative. Hence, (I_v^*, I_h^*) is LAS in $\mathcal{D}_d$ if $\mathcal{R}_0 > 1$.

Moreover, let us denote

$$\begin{pmatrix} h_1(I_v, I_h) \\ h_2(I_v, I_h) \end{pmatrix} \triangleq \begin{pmatrix} \frac{ba}{N_h}(N_v^* - I_v)I_h - \frac{mI_v}{n+N_v^*}N_h - \mu_v I_v \\ \frac{ca}{N_h}I_v(N_h - I_h) + p\frac{mI_v}{n+N_v^*}(N_h - I_h) - \mu_h I_h \end{pmatrix}$$

and

$$\frac{\partial h_1}{\partial I_v} + \frac{\partial h_2}{\partial I_h} = -ba\frac{I_h}{N_h} - \frac{mN_h}{n+N_v^*} - \mu_v - \frac{ca}{N_h}I_v - \frac{pmI_v}{n+N_v^*} - \mu_h < 0.$$

Thus, system (3.8) has no periodic orbits $\mathcal{D}_d$. By Poincaré-Bendixson Theorem in [15], the single equilibrium (I_v^*, I_h^*) is GAS in $\mathcal{D}_d$ if $\mathcal{R}_0 > 1$. Hence, the unique endemic equilibrium E_e is also GAS in $\mathcal{D}$ if $\mathcal{R}_v > 1$ and $\mathcal{R}_0 > 1$. □

Theorem 3.6. *If $\mathcal{R}_v < 1$, system (2.1) has up to five equilibria:*

$$E_0 = (0, 0, 0),\ E_{b^\pm} = (N_{v^\pm}^*, 0, 0),\ E_{e^\pm} = (S_{v^\pm}^*, I_{v^\pm}^*, I_{h^\pm}^*).$$

Moreover,

(i) *Suppose $0 < \sigma n < 1 - \frac{\mu_v}{r_v}$ and $m_l < m < m_u$, we have*
   (a) *if $\mathcal{R}_0(N_{v^-}^*) < \mathcal{R}_0(N_{v^+}^*) < 1$, then E_0 and $E_{b^\pm}$ exist. Moreover, both E_0 and E_{b^+} are LAS, and E_{b^-} is unstable in $\mathcal{D}$.*

(b) *if* $\mathcal{R}_0(N^*_{v^-}) < 1 < \mathcal{R}_0(N^*_{v^+})$, *then* $E_0, E_{b^\pm}$ *and* E_{e^+} *exist. Moreover, both* E_0 *and* E_{e^+} *are LAS, and* $E_{b^\pm}$ *are unstable in* $\mathcal{D}$.

(c) *if* $1 < \mathcal{R}_0(N^*_{v^-}) < \mathcal{R}_0(N^*_{v^+})$, *then* $E_0, E_{b^\pm}$ *and* $E_{e^\pm}$ *exist. Moreover, both* E_0 *and* E_{e^+} *are LAS, and* $E_{b^\pm}, E_{e^-}$ *are unstable in* $\mathcal{D}$.

(ii) *if otherwise, only* E_0 *exists and it is GAS in* $\mathcal{D}$.

Proof. (i) It follows from Theorem 3.2 that both $N^*_{v^-}$ and $N^*_{v^+}$ exist, arising two boundary equilibria E_{b^-} and E_{b^+} of system (2.1), respectively. Since $N^*_{v^-}$ is unstable and N^*_{v0} is LAS in case of $\mathcal{R}_v < 1$, immediately we obtain that E_{b^-} is unstable and E_0 is LAS.

Similar to Theorem 3.5, by setting $S'_v(t) = 0, I'_v(t) = 0$ and $I'_h(t) = 0$ in system (2.1), we obtain

$$I^*_{h^\pm} = \frac{\alpha^\pm\gamma^\pm}{N^*_{v^\pm} + \gamma^\pm}\Big(\mathcal{R}_0^2(N^*_{v^\pm}) - 1\Big) = N_h - \frac{(N_h + \alpha^\pm)\gamma^\pm}{N^*_{v^\pm} + \gamma^\pm}, \tag{3.9}$$

and

$$S^*_{v^\pm} = \frac{\alpha^\pm}{I^*_{h^\pm} + \alpha^\pm} N^*_{v^\pm}, \quad I^*_{v^\pm} = \frac{\gamma^\pm I^*_{h^\pm}}{N_h - I^*_{h^\pm}},$$

where

$$\alpha^\pm = \frac{\frac{mN_h}{n+N^*_{v^\pm}} + \mu_v}{ba/N_h}, \quad \gamma^\pm = \frac{\mu_h N_h}{ca + p\frac{mN_h}{n+N^*_{v^\pm}}}.$$

(a) If $\mathcal{R}_0(N^*_{v^-}) < \mathcal{R}_0(N^*_{v^+}) < 1$. $E_0, E_{b^\pm}$ exist and it is obvious that E_0 is LAS and E_{b^-} is unstable. The Jacobian matrix at E_{b^+} is

$$J\Big|_{E_{b^+}} = \begin{pmatrix} \eta(N^*_{v^+}) & r_v(1-\sigma N^*_{v^+})e^{-\sigma N^*_{v^+}} + \frac{mN_h N^*_{v^+}}{(n+N^*_{v^+})^2} & -\frac{ba}{N_h}N^*_{v^+} \\ 0 & -\frac{mN_h}{n+N^*_{v^+}} - \mu_v & \frac{ba}{N_h}N^*_{v^+} \\ 0 & ca + p\frac{mN_h}{n+N^*_{v^+}} & -\mu_h \end{pmatrix}.$$

One of the eigenvalues is $\lambda_1 = \eta(N^*_{v^+}) \triangleq N^*_{v^+} f_1'(N^*_{v^+}) < 0$. The other two eigenvalues λ_2 and λ_3 are determined by the following equation:

$$\lambda^2 + \Big(\frac{mN_h}{n+N^*_{v^+}} + \mu_v + \mu_h\Big)\lambda + \mu_h\Big(\frac{mN_h}{n+N^*_{v^+}} + \mu_v\Big)\Big(1 - \mathcal{R}_0^2(N^*_{v^+})\Big) = 0. \tag{3.10}$$

Hence, $\mathrm{Re}\big(\lambda(E_{b^+})\big) < 0$ owing to $\mathcal{R}_0(N^*_{v^+}) < 1$, thus E_{b^+} is LAS.

(b) If $\mathcal{R}_0(N^*_{v^-}) < 1 < \mathcal{R}_0(N^*_{v^+})$. Eq. (3.9) implies that E_{e^+} exists. By Eq. (3.10), it implies there exists at least one eigenvalue with a positive real part if $\mathcal{R}_0(N^*_{v^+}) > 1$, indicating E_{b^+} is unstable. Moreover, the Jacobian matrix at E_{e^+} is

$$J(E_{e^+}) = \begin{pmatrix} \eta(N^*_{v^+}) - J_{21} & \eta(N^*_{v^+}) - J_{22} & -J_{23} \\ J_{21} & J_{22} & J_{23} \\ J_{31} & J_{32} & J_{33} \end{pmatrix},$$

where

$$J_{21} = ba\frac{I^*_{h^+}}{N_h} + \frac{mN_h I^*_{v^+}}{(n+N^*_{v^+})^2}, \quad J_{22} = -\Big(\frac{mN_h(n+S^*_{v^+})}{(n+N^*_{v^+})^2} + \mu_v\Big),$$
$$J_{23} = \frac{ba}{N_h}S^*_{v^+}, \quad J_{31} = -p\frac{mI^*_{v^+}(N_h - I^*_{h^+})}{(n+N^*_{v^+})^2},$$
$$J_{32} = \Big(\frac{ca}{N_h} + \frac{pm(n+S^*_{v^+})}{(n+N^*_{v^+})^2}\Big)(N_h - I^*_{h^+}), \quad J_{33} = -\Big(\frac{ca}{N_h}I^*_{v^+} + \frac{pmI^*_{v^+}}{n+N^*_{v^+}} + \mu_h\Big).$$

The characteristic polynomial of $J(E_{e^+})$ is

$$\det\Big(\lambda I - J(E_{e^+})\Big) = \Big(\lambda - \eta(N^*_{v^+})\Big)(\lambda^2 + a_1\lambda + a_2),$$

where

$$a_1 = ba\frac{I^*_{h^+}}{N_h}\frac{N^*_{v^+}}{I^*_{v^+}} + \frac{\mu_h N_h}{N_h - I^*_{h^+}} > 0, \quad a_2 = \mu_h \frac{ba}{N_h}\frac{I^*_{h^+}}{I^*_{v^+}}\frac{N_h I^*_{v^+} + S^*_{v^+} I^*_{h^+}}{N_h - I^*_{v^+}} > 0.$$

The eigenvalues of $J(E_{e^+})$ are $\lambda_1 = \eta(N^*_{v^+}) < 0$, $\mathrm{Re}(\lambda_2) < 0$, $\mathrm{Re}(\lambda_3) < 0$, which yields that the endemic equilibrium E_{e^+} is LAS.

(c) If $1 < \mathcal{R}_0(N^*_{v^-}) < \mathcal{R}_0(N^*_{v^+})$, both E_{e^-} and E_{e^+} exist. By *(b)*, we know that E_{e^+} is LAS and E_{b^+} is unstable. Meanwhile, similar procedure leads to $\lambda_1 = \eta(N^*_{v^-}) \triangleq N^*_{v^-} f_1'(N^*_{v^-}) > 0$ which is one of eigenvalues of $J(E_{e^-})$. Hence, E_{e^-} is unstable.

(ii) Under the associated situations and Theorem 3.2, the unique N^*_{v0} is GAS in $\mathcal{D}_v$ which implies

$$\lim_{t\to+\infty} S_v(t) = \lim_{t\to+\infty} I_v(t) = 0.$$

This leads to $I_h'(t) = -\mu_h I_h(t)$, yielding $I_h(t)$ degenerates zero for any initial nonnegative conditions. Therefore, E_0 is GAS in $\mathcal{D}$. □

Figure 5 shows the bifurcation of endemic equilibria in terms of $\mathcal{R}_0$. As shown in Fig. 5(a) where $\mathcal{R}_v < 1$, if $0 < \sigma n < 1 - \frac{\mu_v}{r_v}, m_l < m < m_u$ are satisfied, a stable endemic equilibrium occurs when $\mathcal{R}_0(N^*_{v^+}) > 1$. With the continuous increase of $\mathcal{R}_0(N^*_{v^+})$, an unstable endemic equilibrium occurs if $\mathcal{R}_0(N^*_{v^-})$ is also greater than unity. However, in case of $\mathcal{R}_v > 1$, the situation is rather simple, namely a unique endemic equilibrium occurs if and only if $\mathcal{R}_0 > 1$ (see Fig. 5(b)).

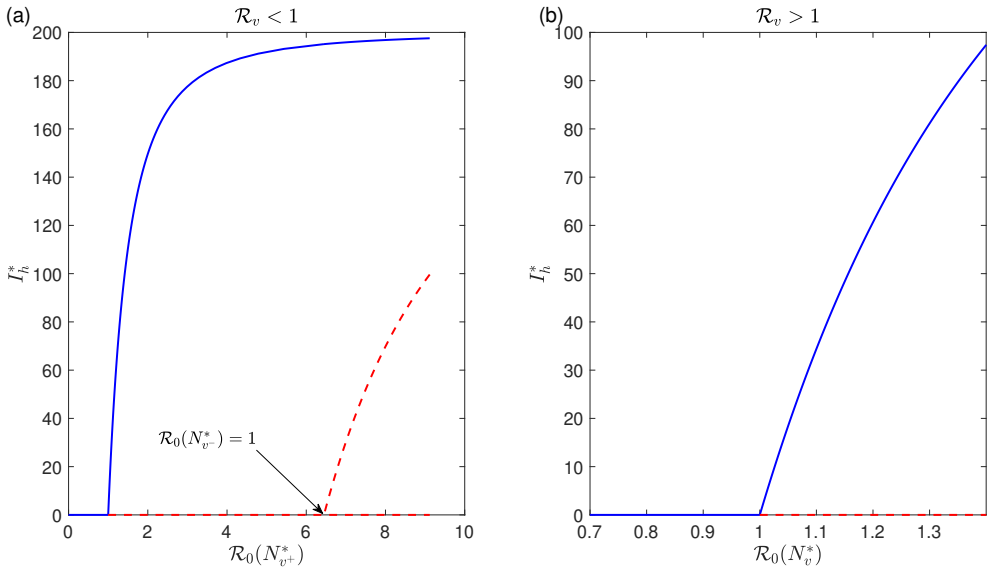

FIGURE 5. Forward bifurcation of system (2.1) in terms of $\mathcal{R}_0$, when (a) $\mathcal{R}_v < 1$, (b) $\mathcal{R}_v > 1$. The blue solid lines indicate stable, while the red dashed lines indicate unstable disease-free or endemic equilibrium.

Remark 3.3. In case of $\mathcal{R}_v < 1$, the backward bifurcation for the vector population in Fig. 4 implies that the triatomine bug population can still persist even if its vector reproduction number is less than

TABLE 2. Summary of equilibria and stability of the model (2.1). '$*$' indicates positive component.

Equilibrium	Feasibility conditions	Stability conditions
$E_0 = (0, 0, 0)$	Always exists	$\mathcal{R}_v < 1$
$E_{b^+} = (*, 0, 0)$	$\mathcal{R}_v < 1, 0 < \sigma n < 1 - \frac{\mu_v}{r_v}, m_l < m < m_u$	$\mathcal{R}_0(N^*_{v^+}) < 1$
$E_{b^-} = (*, 0, 0)$	$\mathcal{R}_v < 1, 0 < \sigma n < 1 - \frac{\mu_v}{r_v}, m_l < m < m_u$	Always unstable
$E_{e^+} = (*, *, *)$	$\mathcal{R}_v < 1, 0 < \sigma n < 1 - \frac{\mu_v}{r_v}, m_l < m < m_u, \mathcal{R}_0(N^*_{v^+}) > 1$	LAS
$E_{e^-} = (*, *, *)$	$\mathcal{R}_v < 1, 0 < \sigma n < 1 - \frac{\mu_v}{r_v}, m_l < m < m_u, \mathcal{R}_0(N^*_{v^-}) > 1$	Always unstable
$E_b = (*, 0, 0)$	$\mathcal{R}_v > 1$	$\mathcal{R}_0(N^*_v) < 1$
$E_e = (*, *, *)$	$\mathcal{R}_v > 1, \mathcal{R}_0(N^*_v) > 1$	GAS

unity. However, the forward bifurcation for the infected population in Fig. 5(a) indicates that Chagas disease can die out if $\mathcal{R}_0(N^*_{v^+}) < 1$, while persists if $\mathcal{R}_0(N^*_{v^+}) > 1$.

4. Numerical Simulations

In this section, we numerically investigate the effect of predation transmission on the transmission of Chagas disease. The selected parameter values are based on Table 1.

4.1. **Bistability if $\mathcal{R}_v < 1$.** With the feasible parameter values chosen from Table 1, we observe different bistability phenomena which are shown in Figure 6, where $\mathcal{R}_v = 0.9472 < 1$. As shown in Fig. 6(a), when $\mathcal{R}_0(N^*_{v^-}) = 0.3094 < \mathcal{R}_0(N^*_{v^+}) = 0.9129 < 1$, both bug-free equilibrium E_0 and disease-free equilibrium E_{b^+} are stable and the other disease-free equilibrium E_{b^-} is unstable, which implies no Chagas disease spreads. However, as depicted in Fig. 6(b,c), either $\mathcal{R}_0(N^*_{v^-}) = 0.5559 < 1 < \mathcal{R}_0(N^*_{v^+}) = 1.6404$ or $1 < \mathcal{R}_0(N^*_{v^-}) = 1.1547 < \mathcal{R}_0(N^*_{v^+}) = 3.4073$, the bug-free equilibrium E_0 and an endemic equilibrium E_{e^+} are synchronously stable, indicating different initial vector-host population may lead to extinction or persistence of Chagas disease if $\mathcal{R}_v < 1$.

4.2. **Global Stability if $\mathcal{R}_v > 1$.** We have shown that, if $\mathcal{R}_v > 1$, the disease-free equilibrium E_b is globally asymptotically stable when $\mathcal{R}_0(N^*_v) < 1$ and an endemic equilibrium E_e is globally asymptotically stable when $\mathcal{R}_0(N^*_v) > 1$ (see Theorem 3.5). Figure 7 presents the intuitive observation of the global stability phenomena, where $\mathcal{R}_v = 1.9867$, $\mathcal{R}_0(N^*_v) = 0.9129$ for (a) and $\mathcal{R}_0(N^*_v) = 1.1952$ for (b). Biologically, even if the vector reproduction number $\mathcal{R}_v > 1$, Chagas disease can either die out if $\mathcal{R}_0 < 1$ or persist if $\mathcal{R}_0 > 1$.

4.3. **Impact of Predation Transmission.** In this subsection, we numerically examine the influence of predation transmission on the transmission of Chagas disease.

Figures 8-9 present the impact of key parameters (n, m, p, N_h) relevant to the predation transmission on the basic reproduction number $\mathcal{R}_0$ of Chagas disease and the number of infected hosts at equilibrium I^*_h in cases of $\mathcal{R}_v > 1$, respectively. It is noticed, increasing the values of predation half-saturation constant n and the predation infection probability p would increase $\mathcal{R}_0$ and I^*_h, whereas increasing the values of the maximum predation rate m and the total number of host population N_h result in the decrease of $\mathcal{R}_0$. It is worthwhile to mention that, within the reasonable parameter ranges, $\mathcal{R}_0$ can either greater than or less than unity.

However, it is interestingly observed as shown in Fig. 9(d), with the increase of N_h, the number of infected hosts I^*_h initially increases at the low level of N_h, reaches peak value and then declines. The

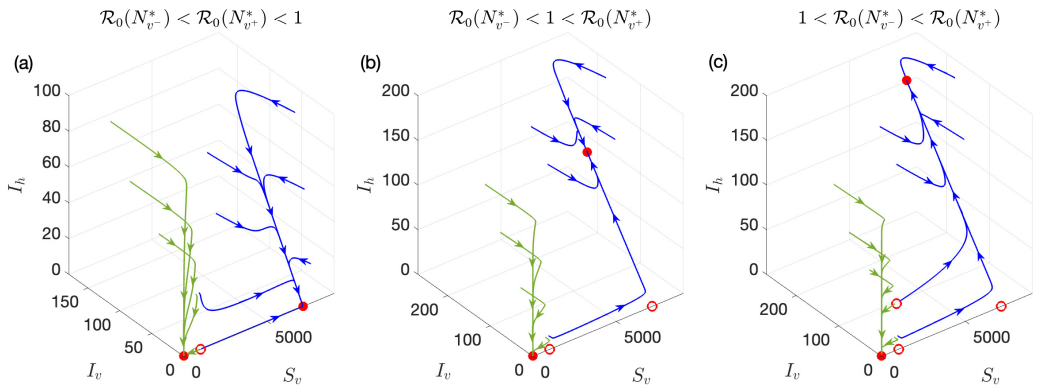

FIGURE 6. Bistability of system (2.1) when $\mathcal{R}_v < 1$. (a) E_0 and E_{b^+} are stable and E_{b^-} is unstable, here $\mu_h = 0.0021$; (b) E_0 and E_{e^+} are stable, and $E_{b^\pm}$ are unstable, here $\mu_h = 0.00064$; (c) E_0 and E_{e^+} are stable, and $E_{b^\pm}$ and E_{e^-} are unstable, here $\mu_h = 0.00025$. Other parameter values are fixed at $a = 0.6$, $b = 0.00471$, $c = 0.00106$, $N_h = 200$, $\sigma = 0.0001$, $r_v = 0.1714$, $\mu_v = 0.0045$, $p = 0.01$, $n = 5842$, $m = 5.1549$. Red solid dots indicate stable and red circles indicate unstable.

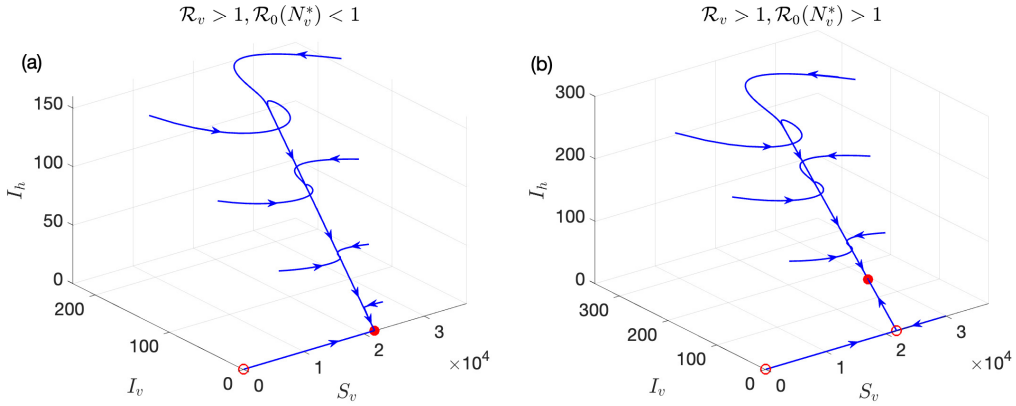

FIGURE 7. Global stability of system (2.1) if $\mathcal{R}_v > 1$ and (a). $\mathcal{R}_0 < 1$, (b). $\mathcal{R}_0 > 1$. Model parameter values are $a = 0.25$, $b = 0.00271$, $c = 0.00106$, $N_h = 200$, $\sigma = 0.0001$, $r_v = 0.6714$, $\mu_v = 0.0045$, $p = 0.01$, $n = 5960$, $m = 9.9365$, $\mu_h = 0.0011$ for (a) and $\mu_h = 0.00067$ for (b).

reason behind may be that the rate of predation transmission exceeds the rate of death due to host predation.

We further conduct sensitivity analysis of model parameters on the basic reproduction number $\mathcal{R}_0$ in case of $\mathcal{R}_v > 1$, by evaluating partial rank correlation coefficients (PRCCs) [17]. Latin hypercube sampling (LHS) is used to sample the parameters from the uniform distribution, with parameters varying from the ranges stated in caption of Figure 10. From the results shown in Fig. 10, we can find that, predation-related parameters m, n, N_h have a notable impact on $\mathcal{R}_0$.

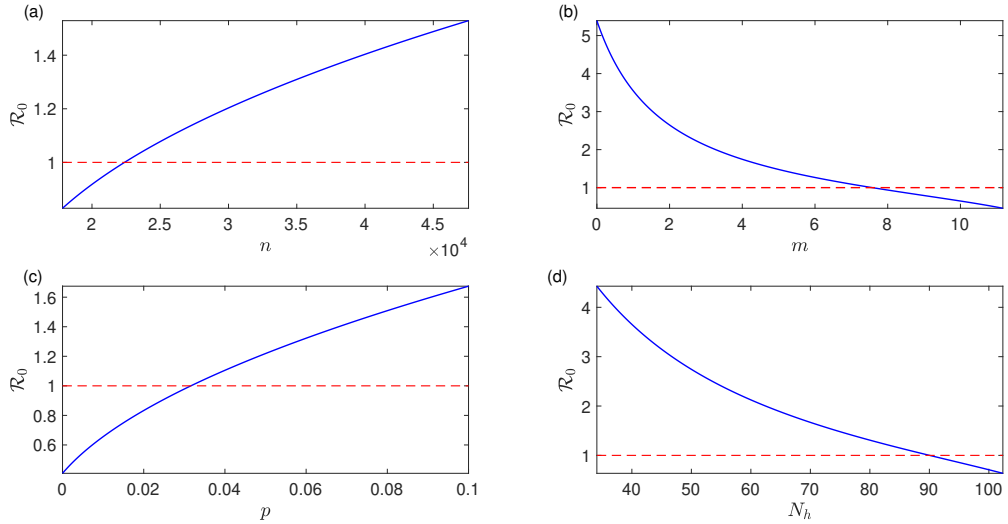

FIGURE 8. The impact of predation transmission parameters n, m, p, N_h on $\mathcal{R}_0$ when $\mathcal{R}_v > 1$. Except for the values of n, m, p, N_h, all other parameter values are the same as those in Fig. 6

.

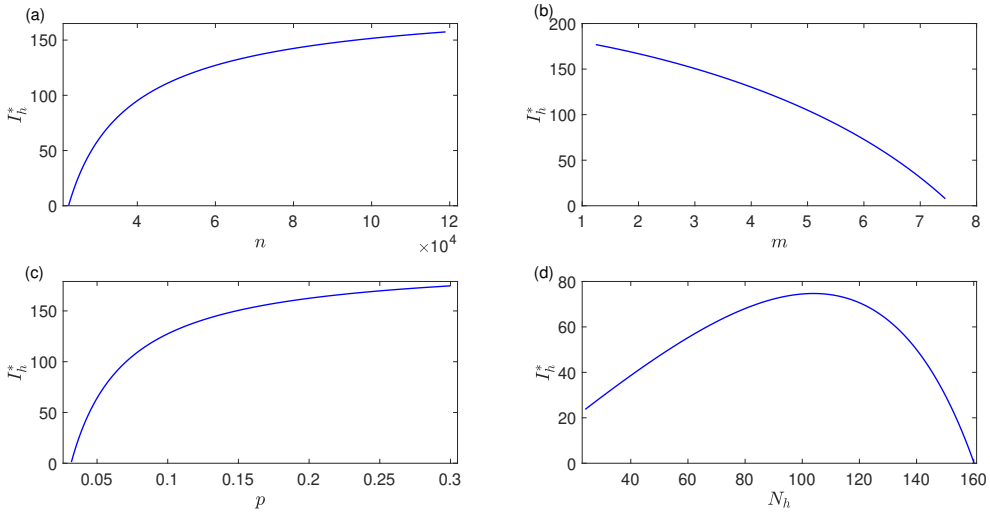

FIGURE 9. The impact of predation transmission parameters n, m, p, N_h on the number of the infected hosts I_h^*. Apart from n, m, p, N_h, the other parameter values are the same as those in Fig. 6

.

4.4. **Contribution of Two Different Transmission Routes.** Since two transmission routes of biting-defecation and predation transmission are involved in model (2.1), we are able to evaluate the respective contributions to basic reproduction number $\mathcal{R}_0$ and newly infected hosts I_h^*. From the formula

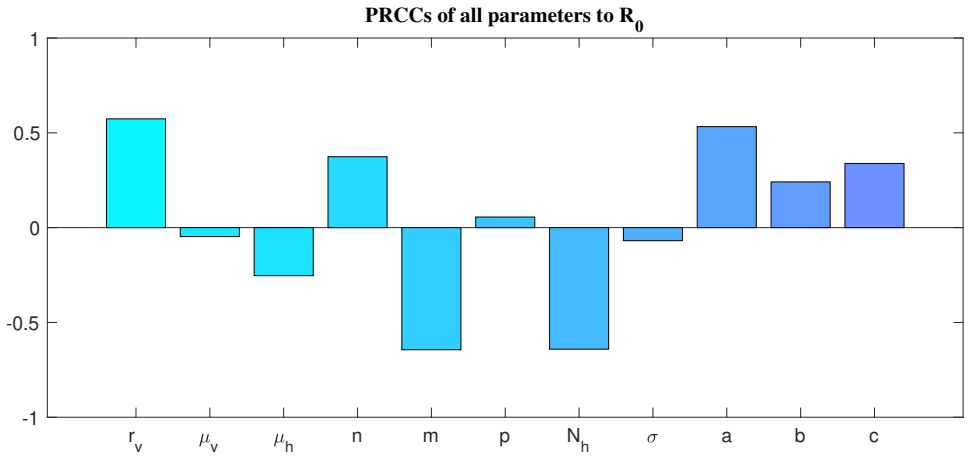

FIGURE 10. PRCCs results of all parameters to the basic reproduction number $\mathcal{R}_0$. The ranges of $a, b, c, r_v, \mu_v, \mu_h, p$ and N_h refer to Table 1. Ranges of n and σ are chosen $\pm 20\%$ at baseline values of $9840, 0.0001$, respectively. The range of m is determined by the existence analysis of the positive equilibrium.

$\mathcal{R}_0$ in Eq. (3.7), their respective percentages to the contribution of $\mathcal{R}_0$ are

$$\widetilde{Q}_b = \frac{\mathcal{R}_b}{\mathcal{R}_0^2} \text{ and } \quad \widetilde{Q}_p = \frac{\mathcal{R}_p}{\mathcal{R}_0^2},$$

and their respective time series percentages to the contribution of the number of newly infected hosts are

$$Q_b(t) = \frac{ca}{ca + p\frac{mN_h}{n+N_v(t)}}, \quad Q_p(t) = \frac{p\frac{mN_h}{n+N_v(t)}}{ca + p\frac{mN_h}{n+N_v(t)}}.$$

The subscripts b, p indicate biting-defecation and predation transmission routes, respectively.

Figure 11 presents the respective percentages ($Q_b(t)$ and $Q_p(t)$), arising from two different transmission mechanisms, by varying m and N_h from high to low values, respectively. As we can see from each column in Fig. 11, the percentage of predation transmission can either greater than or less than 0.5, implying the contribution of predation transmission plays an indispensable role during the course of Chagas disease outbreak. Particularly, we notice that the percentage $Q_p(t)$ of predation transmission contribution decreases as m or N_h decreases, requiring the rational evaluation of model parameter values. Note that, we obtain $\widetilde{Q}_b : \widetilde{Q}_p = Q_b(t) : Q_p(t)$ as $t \to +\infty$ at equilibrium which is colored in grey in Fig. 11, which implies that the relative contributions of two transmission routes to $\mathcal{R}_0$ or the number of newly infected hosts are equal.

5. Conclusion and Discussion

In this study, we present a mathematical model for Chagas disease, where predation transmission between triatomine vectors and non-human hosts are considered and Holling-II functional response is used to describe this predation behavior. The findings from this dynamical analysis offer valuable insights for the prevention and control of Chagas disease, where the conditions for the extinction and persistence of Chagas disease could be identified.

Though the proposed model is simple, the dynamics are not simple, up to five equilibria (see Table 2) are found and bistability phenomenon with backward and forward bifurcations is observed. The key

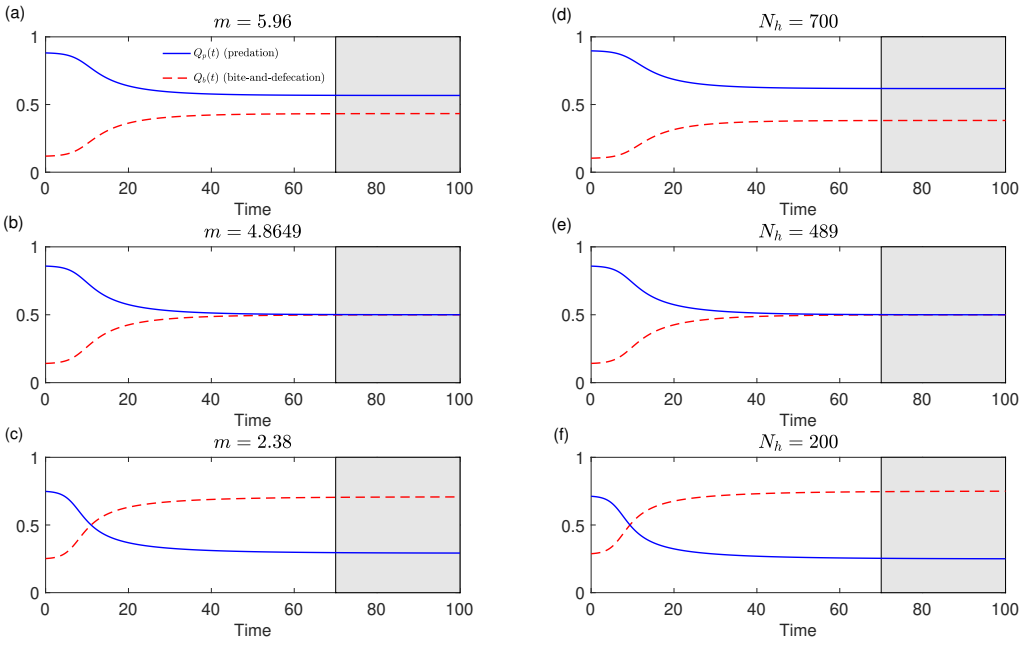

FIGURE 11. The respective percentages of predation transmission and bite-defecation transmission to the contribution of number of new infected hosts by varying m and N_h. Apart from m and N_h, the other parameter values are the same as those in Fig. 7. The grey regions indicate $\widetilde{Q}_b : \widetilde{Q}_p = Q_b(t) : Q_p(t)$ at equilibrium.

findings are that the vector reproduction number $\mathcal{R}_v$ and disease basic reproduction number $\mathcal{R}_0$ are not enough as thresholds to determine the endemicity of Chagas disease. In fact, in case of $\mathcal{R}_v > 1$, the dynamic is simple, namely disease dies out if $\mathcal{R}_0 < 1$ and persists if $\mathcal{R}_0 > 1$. However, in the case of $\mathcal{R}_v < 1$, the dynamic is complicated. Within the biologically feasible ranges of model parameters, i.e. $0 < \sigma n < 1 - \frac{\mu_v}{r_v}$, $m_l < m < m_u$, we have found the backward bifurcation for vector population (Fig. 4) and the forward bifurcation for infected population (Fig. 5), indicating disease still dissipates even if $\mathcal{R}_v < 1$, and different initial conditions or a small perturbation in model parameters may result in a significant variation in the fate of Chagas disease transmission.

With an emphasis on the impact of predation transmission by hosts ingest triatomine bugs on the transmission of Chagas disease, we numerically found that predation transmission basically reduces the risk of infection. We observed that the increase of the maximum predation value m and the number of host population N_h, and the decrease of the half-saturation constant n lead to the decrease of $\mathcal{R}_v$ and $\mathcal{R}_0$, whilst increasing the predation infection probability p results in the increase of $\mathcal{R}_0(N^*_{v\pm})$, see Fig. 8. However, we found unexpectedly that the total number of host population significantly influenced the infected host population. That is, I^*_h initially increases, reaches a peak value and then decreases as N_h increases. Sensitivity analysis stated that model parameters relevant to predation transmission significantly influence $\mathcal{R}_0$. Moreover, the analysis of relative contribution indicated that predation transmission plays an indispensable role in the transmission of Chagas disease. Hence, by increasing the number of host population in an environment and vaccinating hosts which can reduce predation

infection probability may be the practically feasible strategies for the prevention and control of Chagas disease.

There are some limitations with the current study. Human population is not taken account into the model (2.1) for the sake of simplicity, though human is the most important population that should be examined, while the findings from the interplay between triatomines and non-human primates still offer certain valuable insights for the prevention and control of Chagas disease. Secondly, triatomine bugs who are infected with Chagas-parasites have different behavioral activity compared to susceptible triatomine bugs, and non-human primates, like dogs, carrying Chagas-parasites may also have clinical symptoms leading to death [9, 16]. These factors may lead to a significant disparity from the actual situation of this dynamical analysis. Our previous studies have contemplated the factor of pathogenic effect of secondary Chagas-parasite *Trypanosoma rangeli* on the transmission dynamics of Chagas disease, including either co-feeding or co-infection [32, 33]. These factors can be further incorporated into the present model, and we leave these questions for our future investigation.

Declaration of Competing Interest

The authors declare that they do not have financial or non-financial conflict of interests.

Acknowledgments

The authors would like to thank the anonymous reviewers for careful reading and valuable suggestions which help us improve the quality of this paper. We also thank the financial support from the National Science Foundation of China (12271346, 12071300).

Appendix A. Proof of Theorem 3.2

Following Eq. (3.2), we have

$$f_1(0) = (\tfrac{mN_h}{n} + \mu_v)(\mathcal{R}_v - 1), \quad \lim_{N_v \to +\infty} f_1(N_v) = -\mu_v < 0,$$

implying

$$f_1(0) > 0 \Leftrightarrow \mathcal{R}_v > 1, \quad f_1(0) < 0 \Leftrightarrow \mathcal{R}_v < 1.$$

(i) If $\mathcal{R}_v > 1 \Leftrightarrow f_1(0) > 0$.

If $\sigma n \geq 2$, we have

$$g(0) = \sigma n \frac{r_v}{mN_h/n} > \sigma n \frac{r_v}{mN_h/n + \mu_v} = \sigma n \mathcal{R}_v > \sigma n \geq 2.$$

It follows from Lemma 3.1(i) that there is a unique root $\widetilde{N}_{v1} > 0$ such that $g(\widetilde{N}_{v1}) = 1$. This implies that $f_1(N_v)$ directly decreases from the positive value $f_1(0)$ to negative, until converges to $-\mu_v$. Hence, there exists a unique positive equilibrium N_v^* such that $f_1(N_v^*) = 0$.

If $0 < \sigma n < 2$, we have

$$g_{max} = g(\frac{2 - \sigma n}{\sigma}) = \frac{4}{e^2} \cdot \frac{r_v}{mN_h/n} \cdot \frac{e^{\sigma n}}{\sigma n} > \frac{4}{e} \cdot \frac{r_v}{mN_h/n + \mu_v} = \frac{4}{e} \mathcal{R}_v > 1,$$

using

$$\min_{x \in (0,\infty)} \frac{e^x}{x} = e$$

at $x = 1$ and $\mathcal{R}_v > 1$. However, $g(0)$ can either be greater than or less than unity.

If $g(0) \leq 1 < g_{max}$ holds, it follows from Lemma 3.1(ii) that there are two roots $0 < \widetilde{N}_{v1} < \widetilde{N}_{v2}$ such that $g(\widetilde{N}_{v1}) = g(\widetilde{N}_{v2}) = 1$. This indicates that $f_1(N_v)$ increases from positive $f_1(0)$ to a local maximum, then decreases to negative local minimum, increases again, and eventually tends to $-\mu_v$. This situation ensures a unique positive equilibrium N_v^* such that $f_1(N_v^*) = 0$.

If $1 < g(0) < g_{max}$ is satisfied, $f_1(N_v)$ directly decreases to a local minimum and then increases, until converges to $-\mu_v$. This also indicates a unique positive N_v^* such that $f_1(N_v^*) = 0$.

(ii) If $\mathcal{R}_v < 1 \Leftrightarrow f_1(0) < 0$.

If $\sigma n \geq 2$ and $g(0) \leq 1$, it follows from Lemma 3.1(i) and Eq. (3.4) that $f_1(N_v)$ always increases from negative value $f_1(0)$ to negative value $-\mu_v$. If $\sigma n \geq 2$ and $g(0) > 1$, we know that $f_1(N_v)$ decreases first from negative value $f_1(0)$ and then increases to negative value $-\mu_v$. These two cases indicate no roots of $f_1(N_v) = 0$. (See Fig. 3(f,g)).

If $0 < \sigma n < 2$, it follows from Lemma 3.1(i) and Eq. (3.4) that the positive roots of $f_1(N_v)$ depend on three situations: (a). $g(0) \leq 1 < g_{max}$, (b). $g(0) < g_{max} \leq 1$, and (c). $1 < g(0) < g_{max}$.

In case of (a), it is easy to know that $f_1(N_v)$ increases first from negative $f_1(0)$ to a local maximum $f_1(\widetilde{N}_{v1})$, then decreases to a local minimum $f_1(\widetilde{N}_{v2})$ and increases again, eventually converges to negative value $-\mu_v$. This phase transition of f_1 may lead to one equilibrium $N_v^* = \widetilde{N}_{v1} > 0$ if $f_1(\widetilde{N}_{v1}) = 0$, two equilibria $0 < N_{v^-}^* < \widetilde{N}_{v1} < N_{v^+}^* < \widetilde{N}_{v2}$ if $f_1(\widetilde{N}_{v1}) > 0$ and no equilibrium if $f_1(\widetilde{N}_{v1}) < 0$ (See Fig. 3(a,b,c)).

In cases of (b) or (c), it is easy to know that $f_1'(N_v) > 0$ for the former and $f_1'(N_v) < 0$ for $N_v \in [0, \widetilde{N}_{v1})$ and $f_1'(N_v) > 0$ for $N_v \in (\widetilde{N}_{v1}, \infty)$ for the latter. Both cases indicate that no equilibrium exists for $f_1(N_v) = 0$ (See Fig. 3(d,e)).

Next, we will investigate the equivalent conditions for the existence of the two equilibria in terms of model parameters. We consider m as a mutable variable. By some straightforward algebraic calculations, we obtain that the conditions

$$\mathcal{R}_v < 1,\ 0 < \sigma n < 2 \text{ and } g(0) \leq 1 < g_{max}$$

are equivalent to

$$\text{(I)}.\ 0 < \sigma n < 1 - \frac{\mu_v}{r_v}, \quad \frac{n(r_v - \mu_v)}{N_h} < m < \frac{4r_v}{\sigma N_h} e^{\sigma n - 2},$$

or

$$\text{(II)}.\ 1 - \frac{\mu_v}{r_v} \leq \sigma n < 2, \quad \frac{\sigma n^2 r_v}{N_h} \leq m < \frac{4r_v}{\sigma N_h} e^{\sigma n - 2}.$$

To confirm the feasibility of (I) or (II), we need to examine whether the curve of f_1 traverses N_v-axis during the interval $(0, \widetilde{N}_{v1})$. To do this, we first find a critical value of m corresponding to the unique positive equilibrium of model (3.1). Consequently, $f_1(\widetilde{N}_{v1}) = 0$ and $f_1'(\widetilde{N}_{v1}) = 0$ yield

$$\begin{cases} r_v\Big(1 - \sigma(n + \widetilde{N}_{v1})\Big)e^{-\sigma \widetilde{N}_{v1}} - \mu_v = 0, & \text{(A.1a)} \\ m = \dfrac{\mu_v}{N_h} \dfrac{(n + \widetilde{N}_{v1})^2}{\frac{1}{\sigma} - (n + \widetilde{N}_{v1})} > 0, \quad \widetilde{N}_{v1} < \dfrac{2 - \sigma n}{\sigma}. & \text{(A.1b)} \end{cases}$$

Next we should analyze the suitability of Eqs. (A.1).

Let's treat m as a function of $\widetilde{N}_{v1}$. For $\widetilde{N}_{v1} \in (0, (2 - \sigma n)/\sigma)$, Eq. (A.1b) leads to

$$\frac{dm(\widetilde{N}_{v1})}{d\widetilde{N}_{v1}} = \frac{\mu_h}{N_h} \frac{\sigma(n + \widetilde{N}_{v1})}{(\frac{1}{\sigma} - (n + \widetilde{N}_{v1}))^2} \Big(\frac{2 - \sigma n}{\sigma} - \widetilde{N}_{v1}\Big) > 0,$$

implying $m = m(\widetilde{N}_{v1})$ increases monotonically within the interval $(0, (2 - \sigma n)/\sigma)$. We further denote

$$h(\widetilde{N}_{v1}) = r_v\Big(1 - \sigma(n + \widetilde{N}_{v1})\Big)e^{-\sigma \widetilde{N}_{v1}} - \mu_v,$$

then we have

$$\frac{dh(\widetilde{N}_{v1})}{d\widetilde{N}_{v1}} = r_v \sigma^2 e^{-\sigma \widetilde{N}_{v1}} \Big(\widetilde{N}_{v1} - \frac{2 - \sigma n}{\sigma}\Big) < 0,\ \widetilde{N}_{v1} \in (0, \frac{2 - \sigma n}{\sigma}).$$

That is, $h(\widetilde{N}_{v1})$ monotonically decreases with respect to $\widetilde{N}_{v1}$ during the interval $(0, (2-\sigma n)/\sigma)$. Furthermore, we have

$$h\left(\frac{2-\sigma n}{\sigma}\right) = -r_v e^{\sigma n - 2} - \mu_v < 0, \quad h(0) = r_v(1-\sigma n) - \mu_v.$$

To guarantee the positive equilibrium, $h(0) > 0$ is required, which is equivalent to $\sigma n < 1 - \mu_v/r_v$. Therefore, condition (I) holds and (II) is not valid.

Consequently, we conclude that the existence of two positive equilibria for the model (3.1) when $\mathcal{R}_v < 1$ is equivalent to

$$0 < \sigma n < 1 - \frac{\mu_v}{r_v},\ m_l < m < m_u,$$

where

$$m_l = \frac{n(r_v - \mu_v)}{N_h} \ \text{ and } \ m_u = \frac{\mu_v}{\sigma N_h} \frac{\left(1 - W_0(\frac{\mu_v}{r_v} e^{1-\sigma n})\right)^2}{W_0(\frac{\mu_v}{r_v} e^{1-\sigma n})},$$

and W_0 is the principal real branch of transcendent *Lambert W* function.

References

[1] M. A. Acuña-Zegarra, D. Olmos-Liceaga and J. X. Velasco-Hernández, *The role of animal grazing in the spread of Chagas disease*, J. Theor. Biol. **457** (2018), 19-28.

[2] N. F. Britton. *Essential Mathematical Biology*, Springer, New York, 2003.

[3] M. Canals, D. Cáceres, S. Alvarado, A. Canals and P. E. Cattan, *Modeling Chagas disease in Chile: from vector to congenital transmission*, Biosyst. **156** (2017), 63-71.

[4] L. Chen, X. Wu, Y. Xu, and L. Rong, *Modelling the dynamics of Trypanosoma rangeli and triatomine bug with logistic growth of vector and systemic transmission*, Math. Biosci. Eng. **19(8)** (2022), 8452–8478.

[5] D. J. Coffield, A. M. Spagnuolo, M. Shillor, E. Mema, B. Pell, A. Pruzinsky and A. Zetye, *A model for Chagas disease with oral and congenital transmission*, PLoS ONE **8(6)** (2013), e67267.

[6] D. Erazo, J. Cordovez, C. Cabrera, J. E. Calzada, A. Saldana and N. L. Gottdenker, *Modelling the influence of host community composition in a sylvatic Trypanosoma cruzi system*, Parasitology **144(14)** (2017), 1881-1889.

[7] M. Fabrizio, N. J. Schweigmann and N. J. Bartoloni, *Modelling inter-human transmission dynamics of Chagas disease: analysis and application*, Parasitology **141(6)** (2014), 837-848.

[8] R. E. Gürlter and M. V. Cardinal, *Reservoir host competence and the role of domestic and commensal hosts in the transmission of Trypanosoma cruzi*, Acta Trop. **151** (2015), 32-50.

[9] R. E. Gürtler and M. V. Cardinal, *Dogs and their role in the eco-epidemiology of Chagas disease*, Dog Parasites Endangering Human Health **13** (2021), 73-106.

[10] A. M. Jansen, S. C. C. Xavier and A. L. R. Roque, *Trypanosoma cruzi transmission in the wild and its most important reservoir hosts in Brazil*, Parasites Vectors **11(1)** (2018), 502.

[11] C. Kribs-Zaleta, *Vector consumption and contact process caturation in sylvatic transmission of T. cruzi*, Math. Popul. Stud. **13** (2006), 135-152.

[12] C. Kribs-Zaleta, *Estimating contact process saturation in sylvatic transmission of Trypanosoma cruzi in the United States*, PLoS Negl. Trop. Dis. **4(4)** (2010), e656.

[13] C. R. Lazzari, M. H. Pereira and M. G. Lorenzo, *Behavioural biology of Chagas disease vectors*, Mem. Inst. Oswaldo Cruz. **108** (2013), 34-47.

[14] B. Y. Lee, S. M. Bartsch, L. Skrip, D. L. Hertenstein, C. M. Avelis, M. Ndeffo-Mbah, C. Tilchin, E. O. Dumonteil and A. Galvani, *Are the London Declaration's 2020 goals sufficient to control Chagas disease?: modeling scenarios for the Yucatan Peninsula*, PLoS Negl. Trop. Dis. **12(3)** (2018), e0006337.

[15] M. Y. Li, *An Introduction to Mathematical Modeling of Infectious Diseases*, Springer, Switzerland, 2018.

[16] N. P. Marliére, M. G. Lorenzo and A. A. Guarneri, *Trypanosoma cruzi-infected Rhodnius prolixus endure increased predation facilitating parasite transmission to mammal hosts*, PLoS Negl. Trop. Dis. **15(7)** (2021), e0009570.

[17] S. Marione, I. Hogue and C. Ray, *A methodology for performing global uncertainty and sensitivity analysis in systems biology*, J. Theor. Biol. **254(1)** (2008), 178–196.

[18] M. Ndao, N. Kelly, D. Normandin, J. D. Maclean, A. Whiteman, E. Kokoskin, I. Arevalo and B. J. Ward, *Trypanosoma cruzi infection of squirrel monkeys: comparison of blood smear examination, commercial enzyme-linked*

immunosorbent assay, and polymerase chain reaction analysis as screening tests for evaluation of monkey-related injuries, Comp. Med. **50(6)** (2000), 658-665.

[19] Pan American Health Organization, https://www.paho.org/en/topics/Chagas - disease, accessed August 19, 2023.

[20] L. Perko, *Differential Equations and Dynamical Systems*, Springer Science and Business Media, New York, 2013

[21] W. E. Ricker, *Computation and Interpretation of Biological Statistics of Fish Populations*, Department of the Environment, Fisheries and Marine Service, Ottawa, 1975.

[22] F. L. Rocha, A. L. R. Roque, J. S. de Lima, C. C. Cheida, F. G. Lemos, F. C. de Azevedo, R. C. Arrais, D. Bilac, H. M. Herrera and G. Mourão, *Trypanosoma cruzi infection in neotropical wild carnivores (Mammalia: Carnivora): at the top of the T. cruzi transmission chain*, PLoS ONE **8(7)** (2013), e67463.

[23] H. L. Smith, *Monotone Dynamical Systems: An Introduction to the Theory of Competitive and Cooperative Systems*, American Mathematical Society, New York, 1995.

[24] A. M. Spagnuolo, M. Shillor and G. A. Stryker, *A model for Chagas disease with controlled spraying*, J. Biol. Dyn. **5(4)** (2011), 299-317.

[25] A. M. Spagnuolo, M. Shillor, L. Kingsland, A. Thatcher, M. Toeniskoetter and B. Wood, *A logistic delay differential equation model for Chagas disease with interrupted spraying schedules*, J. Biol. Dyn. **6(2)** (2012), 377-394.

[26] H. R. Thieme, *Convergence results and a Poincaré-Bendixson trichotomy for asymptotically autonomous differential equations*, J. Math. Biol. **30(7)** (1992), 755-763.

[27] H. R. Thieme, *Asymptotically autonomous differential equations in the plane*, Rocky Mt. J. Math. **24(1)** (1994), 351-380.

[28] N. Tomasini, P. G. Ragone, S. Gourbière, J. P. Aparicio and P. Diosque, *Epidemiological modeling of Trypanosoma cruzi: low stercorarian transmission and failure of host adaptive immunity explain the frequency of mixed infections in humans*, PLoS Comput. Biol. **13(5)** (2017), e1005532.

[29] P. van den Driessche and Watmough, *Reproduction numbers and sub-threshold endemic equilibria for compartmental models of disease transmission*, Math. Biosci. **180(1)** (2002), 29-48.

[30] J. X. Velasco-Hernández, *An epidemiological model for the dynamics of Chagas' disease*, Biosyst. **26(2)** (1991), 127-134.

[31] J. X. Velasco-Hernández, *A model for Chagas disease involving transmission by vectors and blood transfusion*, Theor. Popul. Biol. **46** (1994), 1-31.

[32] X. Wu, D. Gao, Z. Song and J. Wu, *Modelling triatomine bug population and Trypanosoma rangeli transmission dynamics: co-feeding, pathogenic effect and linkage with chagas disease*, Math. Biosci. **324** (2020), 108326.

[33] X. Wu, D. Gao, Z. Song and J. Wu, *Modelling Trypanosoma cruzi-Trypanosoma rangeli co-infection and pathogenic effect on Chagas disease spread*, Discrete Continuous Dyn. Syst. Ser. B. **28(2)** (2023), 1024-1045.

J. Jiang, School of Science, Shanghai Maritime University, Shanghai, 201306, P. R. China.
Email address: `april.jiahao.jiang@gmail.com`

D. Gao, Department of Mathematics and Statistics, Cleveland State University, Cleveland, 44115, OH, USA.
Email address: `d.gao51@csuohio.edu`

J. Jiang, School of Science, Shanghai Maritime University, Shanghai, 201306, P. R. China.
Email address: `jiaojiang@shmtu.edu.cn`

X. Wu, corresponding author, School of Science, Shanghai Maritime University, Shanghai, 201306, P. R. China.
Email address: `xtwu@shmtu.edu.cn`